

Maximally Confined High-Speed Second-Order Silicon Microdisk Switches

Michael R. Watts, Douglas C. Trotter, and Ralph W. Young
 Sandia National Labs, P.O. Box 5800, Albuquerque New Mexico 87185
 mwatts@sandia.gov

Abstract: We demonstrate the first high-speed second-order silicon microdisk bandpass switch. The switch, constructed of a pair of $3\mu\text{m}$ radii active microdisks possesses $\sim 40\text{GHz}$ flat-top passbands, a 4.2THz free-spectral-range, and a 2.4ns switching time.

©2008 Optical Society of America

OCIS codes: (130.3120) Integrated optics devices; (230.4110) Modulators; (230.5750) Resonators

1. Introduction

As optical networks move from long-distance to short-reach applications, the need for high-speed, low-power, and densely interconnected optical switches becomes increasingly important. Recently, compact, high-speed, broadband Mach-Zehnder switches have been demonstrated in silicon [1,2]. However, many important applications, including supercomputers and intrachip networks, require fine-grain routing of data. Channel selective switches can provide the necessary granularity. Yet, to date, only first order modulators/switches have been constructed in silicon [3,4]. Such devices have Lorentzian band-passes that are unsuitable for the channel-selective switch application. Moreover, all such devices demonstrated to date require ridge waveguides limiting the modal confinement and resulting in small free-spectral-ranges (FSRs). These small FSRs limit the available communication line bandwidth.

Here, we present the results of the first high-speed silicon microphotonic channel-selective-switch. The switch demonstrates flat-top, 2nd-order $\sim 40\text{-GHz}$ pass-bands. Using a new active microdisk design with a hard outer wall, we achieve disk radii of only $R = 3\mu\text{m}$ enabling a 4.2THz FSR and a switching time of 2.4ns . Open eye-diagrams of 10Gb/s pseudo-random bit-streams are demonstrated in both states of the switch with $\geq 16\text{dB}$ on-off extinction.

2. Discussion and Experimental Results

A diagram and scanning electron micrograph (SEM) of a focused ion beam (FIB) cut through the center of the second-order silicon microdisk switch are presented in Fig. 1a and 1b, respectively. The switch consists of a pair of

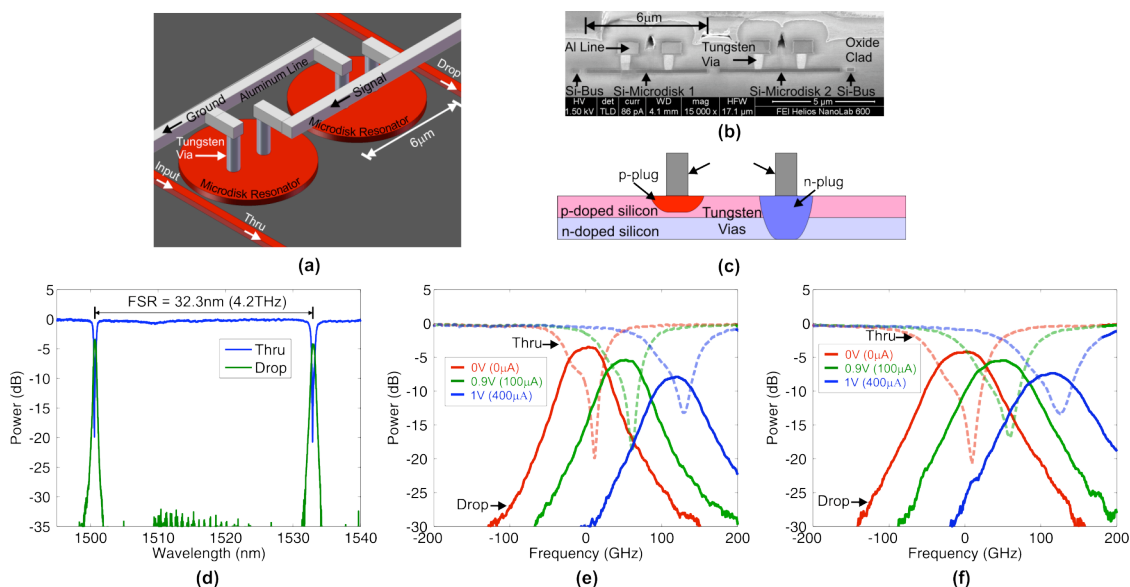


Figure 1. (a) Diagram of the fabricated 2nd order microdisk switch. (b) Scanning electron micrograph (SEM) image of a focused ion beam (FIB) cut through the center of the silicon microdisk switch. (c) Doping profile within microdisk switch. (d) Measured FSR of the 2nd order microdisk switch indicating FSR = 4.2-THz (32.5nm). (e) Measured spectral response of 2nd order microdisk switch as a function of applied voltage ($\lambda_0 = 1501\text{nm}$). The Drop port response has a 33-GHz 1-dB pass-band. (f) Measured spectral response of 2nd order microdisk switch as a function of applied voltage ($\lambda_0 = 1533\text{nm}$). The Drop port response has a 46-GHz 1-dB pass-band.

PDP14.pdf

$R=3\mu\text{m}$ radius microdisk resonators coupled together to provide a 2nd-order filter response. The switch operates on the free-carrier-effect [5] in silicon and the vertical p-n junction used to inject and deplete carriers is depicted in Fig. 1c. By using a vertical junction and making contact from within the center of the disk, all contacts were kept within the interior of the microdisk enabling a hard outer silicon wall of the microdisk to be maintained. This is in contrast to all previously demonstrated silicon microring or microdisk modulators and it is this hard outer wall that enables maximum confinement of the whispering gallery mode with the realized $3\mu\text{m}$ bend radius. Further, the small resonator size enables the massive 4.2-THz demonstrated FSR (see Fig. 1d) critical for maximizing communication line bandwidth. While the switch can be operated at very high speeds ($\tau = 120\text{ps}$) in a reverse-biased mode, wherein carriers are depleted, current doping levels are insufficient to provide the requisite $>40\text{GHz}$ shift required to move the pass-band out of the way. To achieve such a large shift, carriers are injected into the structure by forward biasing the diode. Plots of the filter Thru and Drop port responses at $\lambda_0 = 1501\text{nm}$ and $\lambda_0 = 1533\text{nm}$ as a function of the drive current (and voltage) are provided in Fig. 1e and 1f, respectively. Both resonances demonstrate high-quality second-order filter responses with the corresponding second-order filter roll-off. The filter response shifts to higher frequencies with applied current. Frequency shifts of 50GHz and 117GHz are achieved with applied currents of $100\mu\text{A}$ and $400\mu\text{A}$, respectively. At an applied current of $400\mu\text{A}$, an extinction in the Drop port of $>25\text{dB}$ is achieved at $\lambda_0 = 1501\text{nm}$ and $>20\text{dB}$ at $\lambda_0 = 1533\text{nm}$. Importantly, the filter shape at each resonance is maintained largely independent of the applied bias. The 1-dB passband at $\lambda_0 = 1501\text{nm}$ is 33-GHz wide and the filter achieves peak extinction of 20dB in the Thru port. The 1-dB passband at $\lambda_0 = 1533\text{nm}$ is 46-GHz wide and the filter achieves peak extinction of 20dB in the Thru port. Drop port losses for the $\lambda_0 = 1501\text{nm}$ and $\lambda_0 = 1533\text{nm}$ resonances are 3.5dB and 4dB, respectively. The Drop port loss is a result of several effects including bus-to-disk coupling loss, coupling to the substrate, and to a small extent free-carrier loss. A slight asymmetry exists in the filter Thru and Drop port responses as a result of a small mismatch in the microdisk frequencies. This asymmetry was systematic (a positive slope from low-to-high frequency on all fabricated devices) and likely a result of mechanical or optical loading of the asymmetrically laid out metal contacts.

The switch was fabricated from a silicon-on-insulator (SOI) wafer with an initial 260nm silicon layer thickness and $1\mu\text{m}$ of buried oxide. The realized bus waveguide dimensions were $245\text{nm}\times 360\text{nm}$, and the separations between the bus waveguides and the disk and between the disks were 285nm and 580nm, respectively, as measured by a scanning electron microscope (SEM). The switch geometry was defined with an ASML Deep Ultra-Violet (DUV) laser scanner and silicon reactive ion etch. Sacrificial oxidation was performed at 950°C to remove etch damage and a secondary high temperature (1100°C) oxidation step was performed to passivate the silicon sidewall in preparation for implantation. Subsequently, the diode implants for both the *n* and *p* portions of the junction were performed, followed by *n*+ and *p*+ plugs. Doping concentrations for the diode implants were $5\cdot 10^{17}\text{cm}^{-3}$ and 10^{21}cm^{-3} for the plugs. An anneal at 900°C was used to activate and provide inert ambient for diode passivation to be performed. Finally, a 1.6 μm thick PE-TEOS (plasma enhanced tetraethyl orthosilicate) oxide was deposited and chemical mechanical polished back to 0.9 μm prior to via contact. Low resistance contacts were made by contact titanium sputter, silicidation, and tungsten fill. Finally, a chemical mechanical polish (CMP) was performed followed by a titanium/titanium-nitride/aluminum-copper/titanium-nitride stack for interconnect and contact pads.

The switch operation was demonstrated on a 10-Gb/s 2³¹-1 non-return-to-zero (NRZ) Pseudo Random Bit Stream (PRBS) driving a lithium niobate Mach-Zehnder modulator. The source was a tunable laser set to 1533nm. The data rate was limited by available test equipment. The switch was activated with a 0.57V supplied square-wave through a ground-signal-ground (GSG) microwave probe. The probe was not terminated. Since the switch impedance is substantially larger than 50Ω , reflection at the device nearly doubles the applied voltage. The switch state is switched every 6.4ns in square wave fashion and the Thru port response is depicted in Fig. 2a and 2b. An extinction of 16dB was measured in the Thru port and the switch 10-to-90 percent switch time was measured to be 2.4ns. An eye-diagram of the transmitted data in the Thru port is shown in Fig. 2c. The synchronous measured switch response in the Drop port is shown in Fig. 2d and 2e. An extinction of 20dB was measured in the Drop port and along with a 10-to-90 percent switch response of 2.4ns. An eye diagram of the 10-Gb/s data stream transmitted through the switch to the Drop port is shown in Fig. 2f. The open eye diagrams demonstrate that data integrity is maintained through both states and ports of the switch.

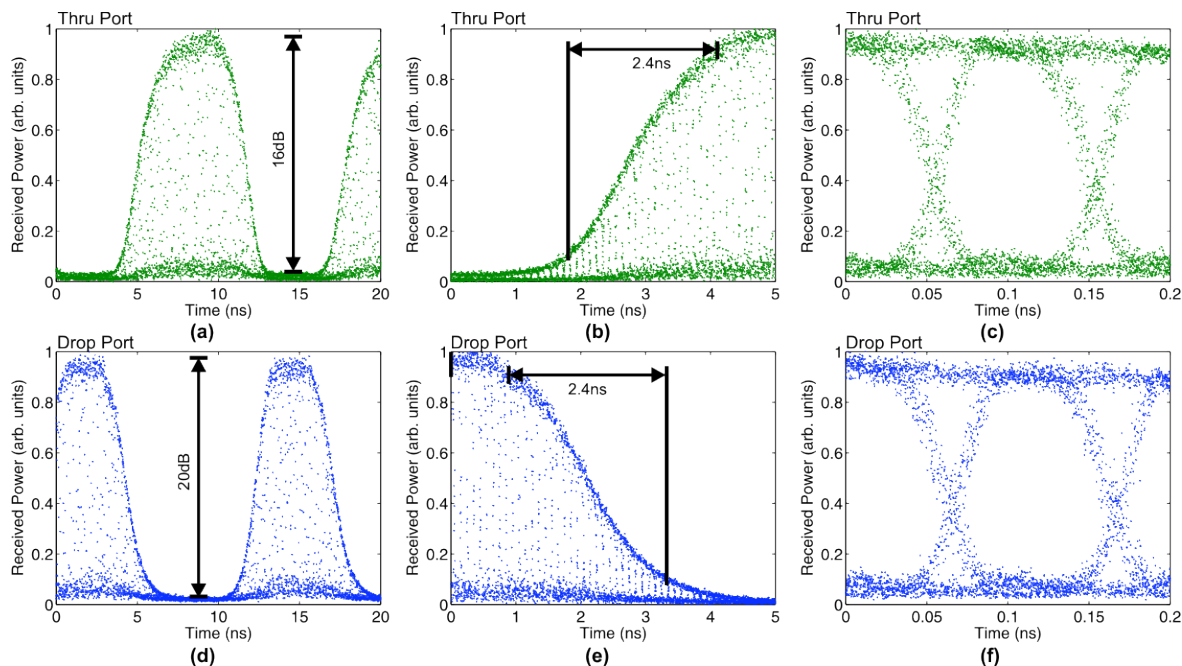


Figure 2. (a) Thru port output versus time switching a 10Gb/s data stream every 6.4ns demonstrating an extinction of -16dB. (b) A close-up of the switch transition in the Thru port indicating a 10-to-90% rise time of 2.4ns. (c) Eye-diagram of the 10Gb/s data stream transmitted at the output of the Thru port of the switch. (d) Synchronous Drop port output versus time with 10Gb/s data stream switched every 6.4ns demonstrating an extinction -20dB. (e) A close-up of the switch transition in the Drop port indicating a 90-to-10% fall time of 2.4ns. (f) Eye-diagram of the 10Gb/s data stream transmitted at the output of the Drop port of the switch.

In supercomputer networks, the physical latency between nodes is often many nanoseconds and the latencies introduced by communication protocols are much greater. The 2.4ns switching speed offered by this channel selective switch corresponds to the physical latency induced by only $\frac{1}{2}$ meter of optical fiber. While intrachip networks may require higher speed switches, 2.4ns is sufficient for applications with short lengths of fiber between nodes. Still, achieving higher speeds is possible and can be achieved with even smaller active microring and microdisk resonators, or alternatively, with more careful design of the dopant distributions within the structure. Further, reverse-biased operation offers innately higher speeds on account of reduced resistance and capacitance. In the present structure, the reverse-biased mode is almost an order of magnitude faster ($\tau=120\text{ps}$) than the forward-biased approach taken here. The challenge is in achieving a sufficiently large reverse-bias induced frequency shift.

3. Conclusions

The first high-speed, 2nd-order, silicon microdisk channel selective switch has been demonstrated. The switch achieves a switching speed of 2.4ns with a flat-top $\sim 40\text{GHz}$ filter bandpass and 20dB extinction in the Thru port. The realized extinction in switching 10Gb/s data stream is 16dB in the Thru port and 20dB in the Drop port. The switch is constructed of the smallest active microdisk resonators demonstrated to date with a radius of $R=3\mu\text{m}$. The small size enables a massive 4.2THz (32nm) FSR that covers the C-band and could enable upto 40+ channels with a 100-GHz channel separation to be integrated onto a single 4-port switch. This small, high-speed, low-power switch forms the building block for richly interconnected short-range optical networks such as the three-dimensional mesh networks connecting high-performance supercomputers.

Partial funding for this work was provided by the DARPA's Microsystems Technology Office (MTO). Sandia is a multiprogram laboratory operated by Sandia Corporation, a Lockheed Martin Company, for the United States Department of Energy's National Nuclear Security Administration under contract DE-AC04-94AL85000.

4. References

1. William M. Green, Michael J. Rooks, Lidija Sekaric, and Yurii A. Vlasov, *Optics Express*, **15**, p. 17106 (2007)
2. A. Liu, R. Jones, L. Liao, D. Samara-Rubio, D. Rubin, O. Cohen, R. Nicolaescu, and M. Paniccia, "A high-speed silicon optical modulator based on a metal-oxide-semiconductor capacitor," *Nature* **427**, 615-618 (2004)
3. Q. Xu, B. Schmidt, S. Pradhan and M. Lipson, "Micrometre-scale silicon electro-optic modulator," *Nature* **435**, 325-327 (2005)
4. C. Gunn, Paper 6125-1, Photonics West, San Jose, January 2006, *Proceedings of SPIE* Vol. #6125
5. R. A. Soref, and B. R. Bennett, "Electrooptical Effects in Silicon," *IEEE J. Quantum Electronics*, **QE-23**, pp. 123-129 (1987)